Check for updates

Received: 4 March 2021 | Accepted: 15 July 2021

DOI: 10.1111/1365-2435.13891

RESEARCH ARTICLE

Functional Ecology | BRITISH ECOLOGICAL SOCIETY

Defoliated trees die below a critical threshold of stored carbon

Audrey Barker Plotkin[1,2] | Meghan Blumstein[3] | Danelle Laflower[1] | Valerie J. Pasquarella[4] | Jennifer L. Chandler[2] | Joseph S. Elkinton[2] | Jonathan R. Thompson[1]

[1]Harvard Forest, Harvard University, Petersham, MA, USA

[2]Department of Environmental Conservation, University of Massachusetts, Amherst, MA, USA

[3]Civil and Environmental Engineering, Massachusetts Institute of Technology, Cambridge, MA, USA

[4]Department of Earth & Environment, Boston University, Boston, MA, USA

Correspondence
Audrey Barker Plotkin
Email: aabarker@fas.harvard.edu

Funding information
Division of Biological Infrastructure, Grant/Award Number: 1459519; Division of Environmental Biology, Grant/Award Number: 1832210 and 1926052

Handling Editor: Katherine McCulloh

Abstract

1. Carbon starvation posits that defoliation- and drought-induced mortality results from drawing down stored non-structural carbohydrates (NSCs), but evidence is mixed, and few studies evaluate mortality directly. We tested the relationships among defoliation severity, NSC drawdown and tree mortality by measuring NSCs in mature oak trees defoliated by an invasive insect, *Lymantria dispar*, across a natural gradient of defoliation severity.
2. We collected stem and root samples from mature oaks (*Quercus rubra* and *Q. alba*) in interior forests ($n = 34$) and forest edges ($n = 47$) in central Massachusetts, USA. Total NSC (TNC; sugar + starch) stores were analysed with respect to tree size, species and defoliation severity, which ranged between 5% and 100%.
3. TNC stores declined significantly with increasingly severe defoliation. Forest edge trees had higher TNC stores that were less sensitive to defoliation than interior forest trees, although this may be a result of differing defoliation history. Furthermore, we observed a mortality threshold of 1.5% dry weight TNC.
4. Our study draws a direct link between insect defoliation and TNC reserves and defines a TNC threshold below which mortality is highly likely. These findings advance understanding and improve model parametrization of tree response to insect outbreaks, an increasing threat with globalization and climate change.

KEYWORDS

carbon starvation, defoliation, *Lymantria dispar* L., non-structural carbohydrates, *Quercus* (oak), tree mortality

1 | INTRODUCTION

Trees rely on stored sugars and starches, collectively termed non-structural carbohydrates (NSCs), for metabolism, transport, defence, osmoregulation and as a buffer during stressful events when photosynthesis is impaired (Dietze et al., 2014; Hartmann & Trumbore, 2016; Martínez-Vilalta et al., 2016; O'Brien et al., 2014; Sapes et al., 2021). Abiotic and biotic disturbances or stressors that limit carbon gain should deplete NSC reserves and lead to death when below a critical level, a process referred to as 'carbon starvation' (McDowell et al., 2008). However, experimental and observational evidence for carbon starvation is mixed. Piper and Paula (2020) synthesized 16 recent studies of NSC response to drought, defoliation and fire under natural conditions. They found lower NSCs in drought-affected *Pinus* species, but few studies and inconsistent results for other stressors. Similarly, in a review of drought mortality (19 studies synthesized in Adams et al., 2017), NSCs sometimes were depleted in trees that died, but often NSC stores were

 © 2021 British Ecological Society

maintained and mortality was better explained by hydraulic failure. Since the carbon starvation hypothesis was originally framed and usually examined in the context of drought, it is challenging to disentangle direct water limitation from carbon depletion, leading to the conclusion that trees typically die of thirst before starvation (Adams et al., 2017).

While drought is an increasing threat to many parts of the globe under climate change, especially the American West (Cohen et al., 2016; Millar & Stephenson, 2015), insect outbreaks are an increasing threat to other forests, especially in the US Northeast and upper Midwest (Aukema et al., 2010; Fei et al., 2019; Liebhold et al., 2013). However, compared to drought, there are few studies of mature tree NSC responses to insect herbivory (Piper & Paula, 2020). Like NSC response to drought, defoliation studies have also found mixed evidence for mortality due to storage depletion. Tree species vary in defoliation tolerance (Kulman, 1971), and many produce a second flush of leaves with high assimilation rates that can compensate for the foliage lost (Heichel & Turner, 1983; Herms et al., 1992). This partially explains why many studies have found that NSC stores remained relatively stable or rebounded quickly following defoliation (Anderegg & Callaway, 2012; Palacio et al., 2012; Piper et al., 2015; Schmid et al., 2017; Wiley et al., 2013), although Landhäusser and Lieffers (2012) found that total NSC root reserves took more than 2 years to recover after herbivory. Notably, none of these defoliation studies included trees that ultimately died or examined the impacts of non-native pest outbreaks, preventing them from directly addressing the role of NSC depletion in mortality and the NSC store level below which recovery was not possible. Understanding what this mortality threshold is for trees is critical to predicting future forest response to infestation.

Here we leverage a natural gradient of defoliation severity and tree mortality to investigate the relationships among defoliation by non-native insect *Lymantria dispar* L. (formerly known as gypsy moth), NSC reserves and tree mortality. *L. dispar* is among the most destructive invasive forest insects in North America (Elkinton & Liebhold, 1990; Lovett et al., 2016). It was a major defoliator in New England during the 20th century but has been quiescent for nearly 30 years. Early work identified a possible threshold for mortality of 2% root starch in young oaks defoliated by *L. dispar* (Wargo, 1981), but no work has been completed since to examine total NSC stores or the impacts to mature trees. We take advantage of a surprisingly severe *L. dispar* outbreak that began in 2016 across southern New England to investigate how depletion of NSC stores may lead to mortality. The outbreak resulted in dramatic mortality of oak (*Quercus* spp.) across thousands of forested hectares by 2018.

Lymantria dispar and its preferred hosts, *Quercus* spp., provide an ideal study system to examine how insect defoliation drives NSC reserve drawdown and mortality. *Quercus* is a globally important genus (Cavender-Bares, 2019) and a dominant in New England forests (Finzi et al., 2020). Furthermore, ring-porous oaks initiate growth and build new xylem prior to bud break each year (Barbaroux & Bréda, 2002; Foster, 2017), making them strongly dependent on reserves of stored NSCs in the spring. *L. dispar* persists at low population densities, punctuated by periodic outbreaks (Elkinton & Liebhold, 1990; Liebhold et al., 2000). Oaks typically can survive 1 or 2 years of defoliation and can produce a second flush of leaves after *L. dispar* larvae pupate in early July (Heichel & Turner, 1983), but mortality risk increases with successive years of defoliation (Davidson et al., 1999), as observed in our study. Infestation levels vary among trees in a stand and among stands, resulting in a natural gradient of defoliation severity (Pasquarella et al., 2018). **We measured survival and NSC stores in oaks that experienced varying defoliation severity and predicted that:**

1. **NSC stores are depleted with increasingly severe defoliation and**
2. **There is a critical NSC threshold below which mortality occurs**.

Following the collapse of the *L. dispar* outbreak in 2018, we measured survival and NSC stores during Winter 2018–2019 (after the final year of defoliation), and again during Winter 2019–2020 to test whether NSC stores recovered in trees that experienced severe defoliation. While some studies have cited rapid recovery of NSCs following defoliation (Palacio et al., 2012; Wiley et al., 2013), other studies observed that recovery took more than 2 years (Landhäusser & Lieffers, 2012; Wiley et al., 2017). We included trees from two distinct habitats—interior forest and roadside trees—because the ecological and economic consequences of pest outbreaks differ between trees in human-dominated landscapes versus forests (Lovett et al., 2016). Forest edge trees receive higher radiation than trees in the forest, which allows for higher leaf area and growth rates (Reinmann & Hutyra, 2017; Reinmann et al., 2020; Smith et al., 2018). Therefore, we predicted that forest edge trees would have higher NSC levels and that NSC stores of forest edge trees would be less sensitive to defoliation than interior forest trees.

2 | MATERIALS AND METHODS

2.1 | Study sites and *L. dispar* outbreak characteristics

In 2016, a major *L. dispar* outbreak began in southern New England, USA, and by 2018 had caused notable oak mortality. Defoliation severity and the number of consecutive years of defoliation were patchy at the regional, site and individual scales. In our central Massachusetts study region, defoliation was widespread in 2017 but more localized in 2016 and 2018 (Elkinton et al., 2019; Pasquarella et al., 2018).

During the mid-late growing season of 2018, we established two study sites. We installed plots in the oak-hardwood forests of the Quabbin Watershed Forest (42.5°N; 72.3°W, hereafter 'Forest'). Northern red oak (*Quercus rubra* L.) was the most common oak species, with some white oak (*Q. alba* L.) and a few black oak (*Q. velutina* Lam.) present. Although *L. dispar* is a generalist herbivore, nearly all the defoliation impacts were observed on *Quercus* and not the other

species in the plots. We chose plots with a range of defoliation severity, based on a published Landsat time series analysis of canopy condition change (Pasquarella, 2018; Pasquarella et al., 2017). Within plots, defoliation of oaks varied. That is, even in lightly defoliated areas, we observed a few oaks that were severely defoliated. We also tagged 85 individual oak trees from roadsides and hedgerows in and within 15 km of the town of Amherst, Massachusetts (42.4°N; 72.5°W, hereafter 'Town'). *Q. rubra* and *Q. alba* were the major oak species present in this site as well. At both sites, for each tree we recorded diameter at breast height (DBH), species and canopy position (1 = full sun; 2 = partially shaded; 3 = mostly/fully shaded). In the Forest plots, we recorded defoliation class (1 = 0%–25% defoliated; 2 = 25%–50% defoliated; 3 = 50%–75% defoliated; 4 = 75%–100% defoliated). For the Town trees, we estimated defoliation to the nearest 5%. These two sites were established independently and came together in Winter 2018–2019 for this study.

To estimate defoliation intensity throughout the *L. dispar* outbreak (2016–2018), we used a Landsat-based condition assessment product (a more recent iteration of the product we used to choose the Forest plots; Pasquarella et al., 2018) that was assessed using a large plot-level defoliation dataset in central Massachusetts (Pasquarella et al., 2021). Change in condition was based on comparison to the best model identified by Pasquarella et al. (2021): a harmonic regression model using a tri-annual frequencies, the Tasseled Cap Greenness spectral index, the full set of Landsat observations (Landsats 5, 7 and 8), a 2005–2015 baseline period and a 1 May–30 September monitoring period. For each tree, we extracted the average condition change score for the 2016, 2017 and 2018 monitoring periods for the Landsat pixel within which the tree was located. The spatial grain of the condition change product (30 m) may encompass canopies of multiple trees, and for the forest edge trees, may include other cover types. Therefore, while this product produces reliable site-level estimates of defoliation intensity, it may not scale well to individual trees.

2.2 | NSC sampling

We selected 34 Forest trees (from four plots) and 47 Town trees for NSC sampling, representing a range of defoliation severity in 2018. All selected trees were alive in late summer 2018, although some were predicted to die within a year based on a visual assessment of crown dieback. Secondary selection criteria included sampling a range of tree size and species. Diameters of the sample trees ranged from 15 to 69 cm at the Forest site (mean 49 cm) and from 12 to 66 cm at the Town site (mean 35 cm). Most of the oaks at the two sites were red oak (*Q. rubra*, $n = 66$) but we included white oak (*Q. alba*, $n = 15$) to the extent it was available.

Non-structural carbohydrate reserves tend to be most stable during the dormant season (Landhäusser & Lieffers, 2003), prior to seasonal drawdown for early stem growth and leaf-out (Furze et al., 2018). Therefore, we sampled NSCs in February 2019, and again in February 2020. From each sample tree, we collected a 2 cm (under bark) sample of wood from (a) the stem, at ~1.3 m height and (b) a coarse root, at ~20 cm from the base of the tree. Samples were collected using a standard 4.3 mm diameter increment borer (Haglöf Company Group), stored on ice in the field, and then stored in a −80°C freezer until processing. We chose to exclude the inner bark, which includes the phloem, as we were largely interested in how longer-term stores are drawn down by defoliation and ultimately impact tree survival rather than current-year photosynthates. We chose to sample from the two largest storage pools in oaks, stems and roots (Furze et al., 2018). While branches are also a significant and dynamic store, we were limited in the location and height of the trees from sampling these tissues.

2.3 | Tree defoliation, dieback and mortality assessments

We assessed defoliation and/or dieback four times over the course of the study. At the initial defoliation assessment in late summer 2018, some of the Forest trees exhibited branch dieback and browning leaves. We recorded crown dieback and mortality status at leaf-out in May 2019, during June–August 2019 and in July–August 2020. A tree was presumed dead if it did not produce leaves; no tree that failed to leaf out in May 2019 produced leaves later that season or in 2020. Crown dieback was rated visually on a five-point scale (1 = 0–25 dieback; 2 = 25%–50% dieback; 3 = 50%–75% dieback; 4 = 75%–99% dieback; 5 = dead). In 2019, we recorded defoliation by *L. dispar* during their larval period from late May–early July. Despite high egg-mass counts in Fall 2018, high larval mortality in 2019 led to very low defoliation (Brown, 2019). There were few *L. dispar* larvae and minimal defoliation in 2020.

2.4 | NSC analysis

Total NSC reserves were extracted from freeze-dried and ground woody tissue samples following the protocol of Landhäusser et al. (2018). In brief, after grinding the wood samples using a Wiley mill and then a ball grinder, we extracted sugars from 30 mg of dried tissue using 80% hot ethanol, then read them using a phenolic colorimetric assay and a spectrophotometer at 490 nm (ThermoFisher Scientific Genesys 180 UV-Vis Spectrophotometer). The methodology extracted and quantified all soluble sugars in the samples, including glucose, sucrose, fructose, and other oligosaccharides and glucans (Landhäusser et al., 2018). We included two internal laboratory standards (*Q. rubra* stem-wood) with each set of samples, with sets within 10% of the laboratory estimate (42 mg/g) accepted.

Starch was extracted from the tissue remaining after sugar extraction using two digestive enzymes: alpha-amylase and amyloglucosidase. Enzymes came in powder form and the amount dissolved into solution depended on the recorded purity of the enzyme batch, to standardize the enzyme activity units per run (Sigma Aldrich code A4551 and ROAMYGLL). We solubilized the tissue in NaOH, then

incubated it at 85°C for 30 min with alpha-amylase dissolved into deionized water, then 55°C for 30 min with amyloglucosidase dissolved in NaOAc buffer solution (25 mM, pH 4.6); both digest starch into glucose. Solutions were assayed using a PGO-colour reagent solution (Sigma Chemicals) and read on the spectrophotometer at 525 nm. Starch concentrations (mg glucose-starch-equivalent per g dry wood) were calculated based on a glucose standard curve (Sigma Chemicals).

2.5 | Data analysis

We used TNC in our analyses, rather than separating the total into the starch and sugar components. We chose to use TNC because we were interested in how the total supply is affected by defoliation, and because sugar and starch content is highly dynamic as they can hydrolyse back and forth in the tree on the order of hours (Tixier et al., 2018). Two of 329 TNC values were negative, with all other values ranging between 0.01% and 11% dry weight. These negative values are the result of zero values with minor error from the laboratory process. Because negative TNC values are biologically impossible, we set the negative TNC values to 10^{-8}%.

Data visualization and analysis were conducted in R version 3.6.1 (R Core Team, 2019). We used a generalized linear mixed modelling (GLMM) approach to analyse the data, using the glmmTMB package (Brooks et al., 2017). To test whether TNC declined with increasing defoliation severity, we analysed the Town and Forest sites separately because we expected edge trees to have higher reserves and therefore more capacity to tolerate defoliation. Fixed effects included 2018 defoliation severity, tree diameter, tree species and canopy exposure. We included diameter to control for the fact that larger trees have larger NSC stores (Sala & Hoch, 2009), and therefore may be more tolerant of defoliation. We included species as a factor because of past evidence for interspecific differences in defoliation effects. For example, a classic paper by Campbell and Sloan (1977) found that *Q. alba* was more heavily defoliated and more likely to die than *Q. rubra*. Although we expected well-lit canopies to have higher resources and more tolerance to defoliation than shaded canopies, canopy exposure was not a significant predictor for either the Forest or Town site, so was not included in the final models. Random effects included year and nested plot/tree/tissue (all Amherst trees were considered one 'plot'). Because TNC is measured as a proportion (percent dry weight), we chose a GLMM with a beta distribution and a logit link (Douma & Weedon, 2019).

To test whether TNC levels predicted tree mortality, we fit a logistic GLMM. We included the Town and Forest sites in the same model because we expected mortality to depend on a critical threshold of TNC regardless of site. Fixed effects included TNC percent and tissue (stem or root). Random effects included year and nested site/plot. For all models, we assessed model fit by examining standardized residuals using the package DHARMa (Hartig, 2020), and extracted model predictions using the package ggeffects (Lüdecke, 2018).

3 | RESULTS

3.1 | Tree characteristics: Defoliation, dieback, mortality and NSCs

Mean defoliation of the sampled trees in 2018 was 30% at the Forest site and 34% at the Town site. Most trees experienced low to moderate defoliation, but 6 of the 34 Forest trees and 13 of the 47 Town trees experienced >50% defoliation. Defoliation was low in 2019; only 6 of the 74 surviving trees had notable (25%–50%) defoliation. Because the study began in 2018, we do not have tree-level estimates of defoliation for 2016 or 2017. Based on the Landsat condition scores, there was minimal defoliation in 2016, and variable levels of defoliation in 2017 and 2018 (Figure 1a–c). The scores were overall lower (more severe defoliation) in 2017 and 2018 for the Forest trees compared to the Town trees (Figure 1e,f); a Welch's two sample *t*-test indicated that mean change in condition was significantly different between the Town and Forest in 2016 ($p = 0.03$), 2017 ($p < 0.001$) and 2018 ($p < 0.001$). However, there was no correlation between the pixel-scale defoliation estimate and the individual-tree defoliation estimate for 2018 (Figure 1g).

During Winter 2018–2019, 7 of the 34 trees in the Forest site died, but no new Forest trees died in Winter 2019–2020. One of the Town trees exhibited near-total crown dieback in Summer 2019. It was cut down between February (after sampling) and August 2020 (when we assessed crown dieback for the Town trees); we coded this tree as 'dead' in 2020. Of the surviving trees, most exhibited low (<25%) crown dieback. At the Forest site, 2 of the 27 surviving trees exhibited 25%–50% dieback in Summer 2019, and this rose to seven trees in Summer 2020. At the Town site, only two surviving trees exhibited >25% dieback in Summers 2019 or 2020.

Total NSC values were higher on average in the Town than the Forest site and declined less in response to defoliation (Figure 2). We observed higher TNC in 2019 than in 2020, and root tissue TNC tended to be higher than stem tissue TNC, especially in 2019 (Table 1). Sugars comprised a larger share of TNC than did starch in our mid-winter sampling (Table 1).

3.2 | Non-structural carbohydrate stores are depleted with increasingly severe defoliation

TNC stores declined with increasing defoliation severity at both sites, but the strength of the relationship varied between sites, as did the influence of tree size and species. The final model for the Forest site showed that TNC stores declined with increasing percent defoliation (Table 2; Figure 2a). Tree diameter was a significant covariate; larger trees had higher TNC. However, there was no significant difference between TNC stores in *Q. rubra* and *Q. alba*. The effect size of defoliation severity was larger than that of tree diameter. The final model for the Town site also showed that TNC

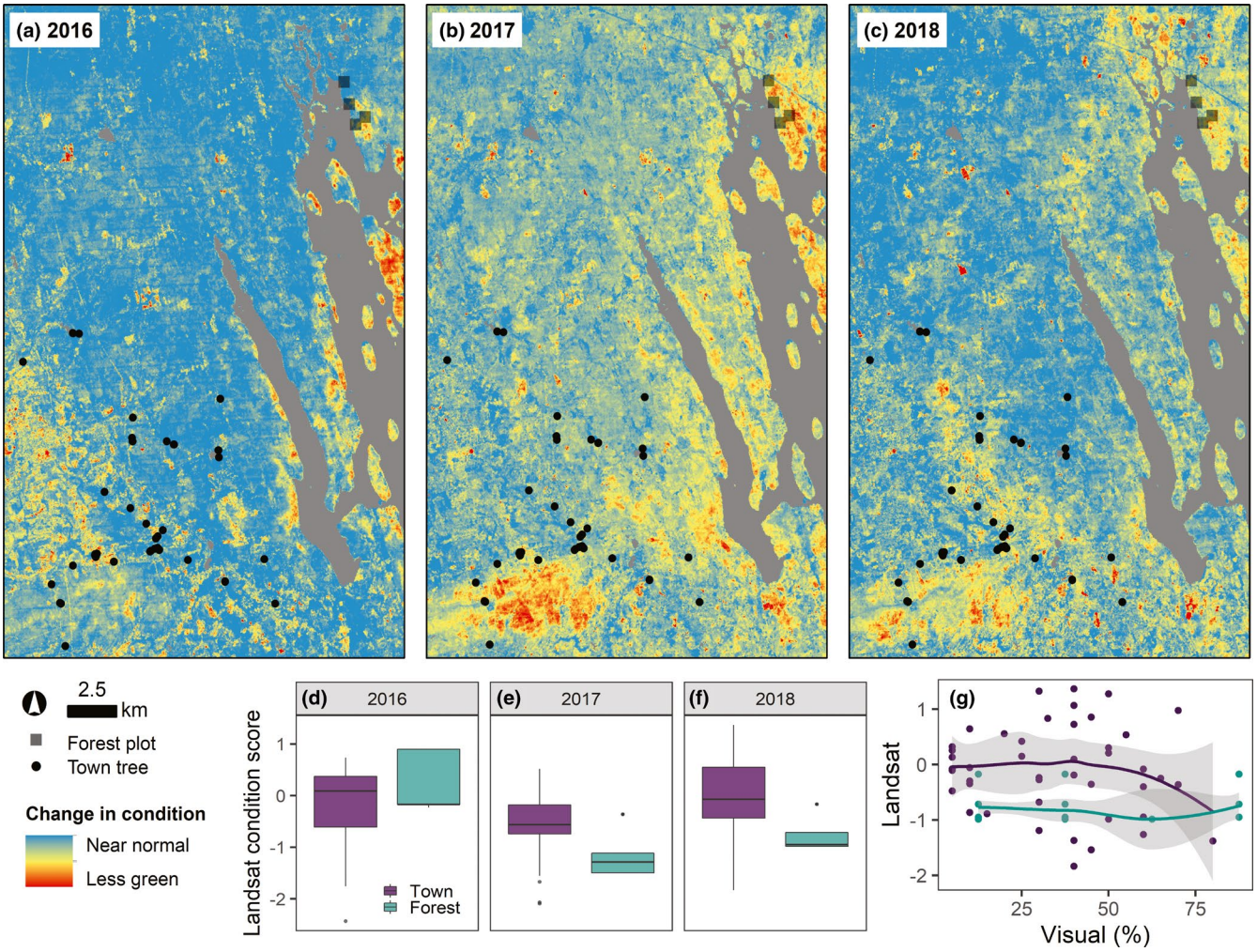

FIGURE 1 (a–c) Estimated forest condition change during the 2016–2018 *Lymantria dispar* outbreak for the central Massachusetts study region, based on Landsat time series analysis (Pasquarella et al., 2021). Note that water is masked in these maps, but non-forest condition change scores are shown; (d–f): distribution of Landsat condition change scores for the Town and Forest trees in 2016, 2017 and 2018. Negative scores indicate less greenness, and positive scores indicate more greenness, compared to a 2005–2015 baseline (Pasquarella et al., 2021); (g) visual estimates of percent defoliation of individual trees ('Visual') in 2018 did not correspond with remote sensing based estimates of defoliation ('Landsat') at the 30 m pixel scale

stores declined with increasing percent defoliation, but the effect size was small compared to the Forest site (Table 2; Figure 2b). Tree diameter was not a significant covariate in the Town model, but *Q. rubra* had significantly higher TNC stores than *Q. alba*.

We also observed interannual variation in average TNC stores; 2019 TNC stores on average were higher than 2020, regardless of defoliation severity. This pattern indicates that NSC stores are also responding to differences in climatic conditions between the two years. 2018 was an unusually wet year (Boose & Gould, 2019), which may explain the overall higher TNC in Winter 2018–2019 than in Winter 2019–2020. We found no evidence that TNC variation between years related to defoliation severity and no evidence of TNC recovery; an interaction term between defoliation and year was non-significant, indicating that TNC difference between 2019 and 2020 was not mediated by defoliation severity.

3.3 | There is a critical non-structural carbohydrate threshold below which mortality occurs

All the trees that died had TNC levels measured the prior February below 1.5% dry weight in root and stem samples (Figure 3). Across sites and years, TNC was a strong predictor of mortality (Table 2; Figure 4) with a sharp increase in survival probability above the 1.5% TNC threshold. This did not differ significantly between stem and root tissue (Table 2).

Surprisingly, eight trees with TNC levels that dropped below the 1.5% threshold survived (Figure 3), all from the Forest site. In 2019, four surviving trees had stem (but not root) TNC levels below 1.5%. One of these three trees again had stem TNC <1.5% in 2020, but the other three trees' stem TNC levels were >1.5%. In 2020, four additional trees had stem and/or root TNC levels <1.5%. These

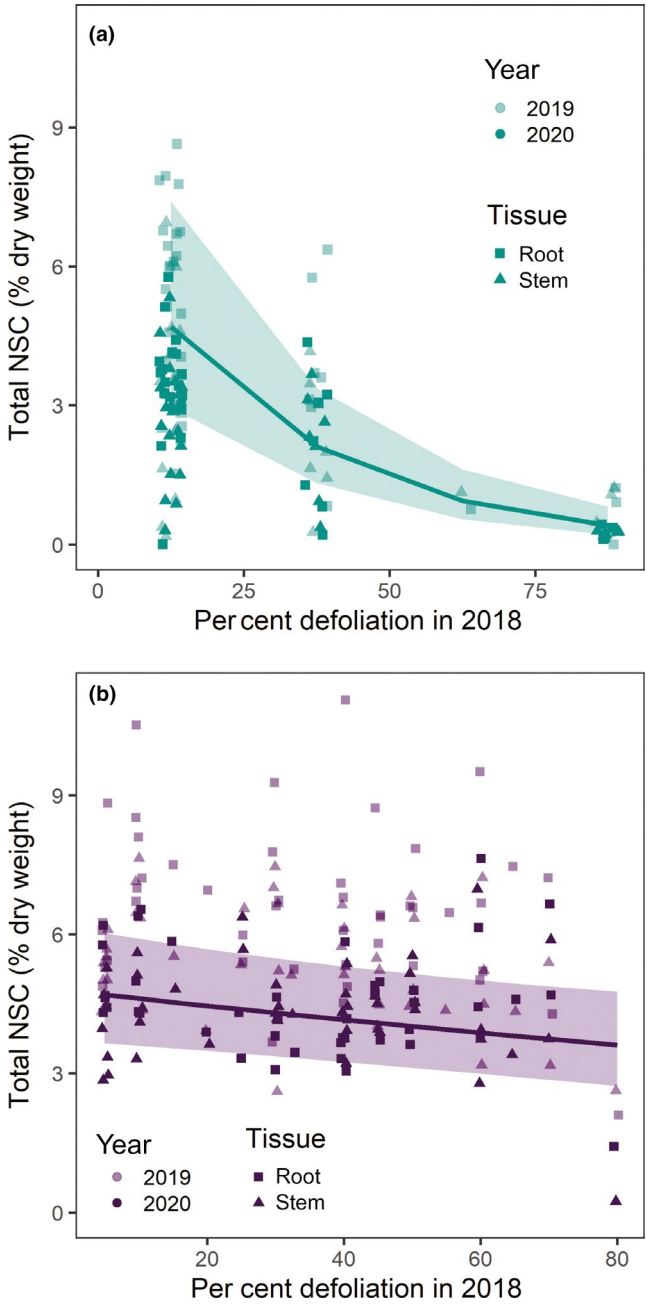

FIGURE 2 Total non-structural carbohydrates (TNC) declined with increasing defoliation severity of oak (*Quercus rubra* and *Q. alba*) by *Lymantria dispar* at the Forest (a) and Town (b) sites. The response was stronger for the Forest site (interior forest trees) than Town site (forest edge trees). The lines and shading show how the predicted TNC amount and 95% CI change with percent defoliation. The points (jittered) show the data

low-TNC survivors did not notably differ from the other surviving trees in terms of species, size or defoliation history. However, five of the eight exhibited 25%–50% crown dieback by 2020 (and only 7 of the 27 surviving trees at the Forest site had 25%–50% crown dieback in 2020), indicating that these low TNC values are likely associated with crown dieback.

4 | DISCUSSION

This study demonstrates that defoliation drives the drawdown of NSC reserves and eventual mortality of trees when defoliation is severe, especially for interior forest trees. These results stand in contrast to studies that have shown weak and transient NSC drawdown in response to defoliation (Palacio et al., 2012; Piper et al., 2015; Piper & Paula, 2020). Furthermore, all the trees that died had root and stem TNC levels <1.5%. Few past studies of NSC response to defoliation included trees that died (Wargo, 1981; Webb, 1981); our study identifies a critical threshold below which mortality is highly likely, directly addressing the role of NSC depletion in mortality.

4.1 | NSC stores are depleted with increasingly severe defoliation, especially in interior forest

We found a significant relationship between defoliation and TNC in both Town and Forest trees, and we found no evidence of recovery one full year after the *L. dispar* outbreak ended. We expect recovery of TNC to take several years and to be influenced by climate and other disturbances (Anderegg, Schwalm, et al., 2015; Landhäusser & Lieffers, 2012). Our study agrees with earlier findings of NSC drawdown following defoliation, including root starch in oaks defoliated by *L. dispar* (Wargo, 1981), stemwood starch in experimentally defoliated oaks (Wiley et al., 2017, though root starch recovered quickly), Douglas-fir defoliated by tussock moth (Webb, 1981) and aspen defoliated by native insects (Landhäusser & Lieffers, 2012). However, experimental defoliation of aspen (Anderegg & Callaway, 2012), defoliation of pine by pine processionary moth (Palacio et al., 2012) and defoliation of *Nothofagus* by *Ormiscodes amphimone* (Piper et al., 2015) found only transient drawdown of NSCs. It is intriguing that most of the studies examined the effects of herbivory by native insects; perhaps non-native insects have a more severe effect on tree carbon stores because the hosts lack an evolutionary history with them (Gandhi & Herms, 2010).

It is unclear why findings differ among studies, especially within the same species. Defoliation history and additional stressors such as drought and competition likely play a part. As conceptualized by the tree mortality spiral, decline and death is a complex, multi-factor process (Franklin et al., 1987; Manion, 1981). Many species are tolerant of a single defoliation event (Kulman, 1971). Most (but not all, e.g. Palacio et al., 2012; Wargo, 1981) prior studies measured NSC drawdown after a single defoliation. In our study, although the defoliation severity of individual trees in 2018 was a much stronger predictor of NSC drawdown than the site-level defoliation history 2016–2018, widespread defoliation in 2017 likely contributed to slow recovery of NSCs. In addition, it is well documented that mortality is greater when *L. dispar* defoliation follows drought (Campbell & Sloan, 1977; Davidson et al., 1999). A drought in 2016 (Koch & Coulton, 2018) as the *L. dispar* outbreak began in central New England likely exacerbated the effects of defoliation in 2016–2018 and contributed to NSC depletion and tree mortality. We

TABLE 1 Non-structural carbohydrate (NSC) levels of the sampled trees by site, tissue and year. The sample size for the Town site differs between years because two healthy oaks (based on their crown vigour ratings in July 2019) were cut down by Town road maintenance workers before the February 2020 sampling

	Forest ($n = 34$)		Town ($n_{2019} = 47$; $n_{2020} = 45$)	
	Root	Stem	Root	Stem
2019 mean % dry weight (*SD*)				
Sugars	3.35 (1.79)	2.00 (1.38)	4.99 (1.18)	3.55 (0.78)
Starch	1.00 (1.15)	0.56 (0.59)	1.61 (1.10)	1.71 (0.85)
Total (TNC)	4.34 (2.56)	2.56 (1.81)	6.60 (1.72)	5.26 (1.24)
2020 mean % dry weight (*SD*)				
Sugars	1.81 (1.24)	1.53 (1.03)	3.46 (0.73)	2.74 (0.77)
Starch	0.80 (0.82)	0.62 (0.66)	1.06 (0.82)	1.58 (0.59)
Total (TNC)	2.61 (1.65)	2.15 (1.43)	4.52 (1.15)	4.32 (1.09)

TABLE 2 Parameter estimates for the fixed effects in the models predicting total non-structural carbohydrate (TNC) and mortality risk. Significant predictors ($p < 0.05$) are in bold. Note that the parameter estimates and standard errors are on the logit scale

Model	Estimate (*SE*)	*p*-value
Forest site. TNC ~		
Intercept	**−3.784 (0.421)**	**<0.001**
Defoliation %	**−0.033 (0.004)**	**<0.001**
DBH	**0.024 (0.008)**	**0.001**
Species (*Q. rubra* relative to *Q. alba*)	−0.303 (0.229)	0.186
Town site. TNC ~		
Intercept	**−2.900 (0.151)**	**<0.001**
Defoliation %	**−0.004 (0.001)**	**0.008**
DBH	−0.003 (0.002)	0.166
Species (*Q. rubra* relative to *Q. alba*)	**0.209 (0.077)**	**0.007**
Survival probability ~		
Intercept	**−3.313 (0.913)**	**<0.001**
TNC (% dry weight)	**2.841 (0.631)**	**<0.001**
Tissue (stem relative to root)	1.166 (0.797)	0.143

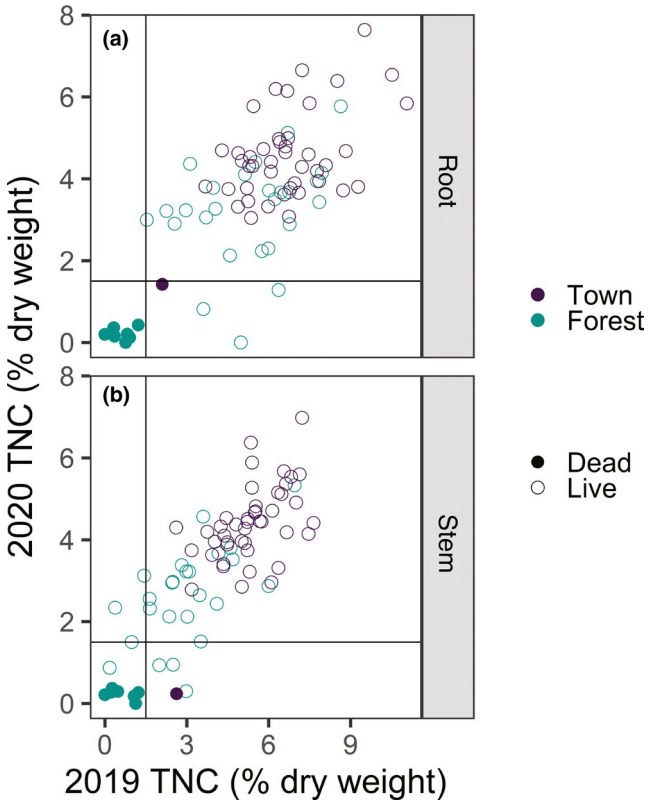

FIGURE 3 Total non-structural carbohydrate (TNC) levels in 2019 and 2020 for Town and Forest trees. Each point is one tree's root (a) or stem (b) sample. All the trees that died had TNC levels that fell below 1.5% dry weight. All the mortality at the Forest site occurred in 2019, whereas the one tree that died at the Town site did so in 2020

did not begin this study until 2018, so could not assess this directly, but a related study (currently in review) found dramatically lower TNC in oaks and other tree species in central New England following the 2016 drought, building on work that showed that NSCs vary among years (Furze et al., 2018; Landhäusser & Lieffers, 2012; Richardson et al., 2013) and that climate is a major driver of interannual variation (Landhäusser & Lieffers, 2012). While 2016 was an unusually dry year in our study area, 2018 was an unusually wet year, which may explain the overall higher TNC in Winter 2018–2019 than in Winter 2019–2020. Recovery may also have been complicated by the fact that trees redistribute nitrogen following a defoliation event (Lovett et al., 2002). Nitrogen redistribution has complex feedbacks on *L. dispar* (Lindroth et al., 1997) and tree performance. In a study that included some of the same tree and forest plot sites, Conrad-Rooney et al. (2020) found lower total soil and leaf N associated with sites defoliated more intensively; low N could limit tree recovery in addition to TNC (Piper et al., 2015).

Another possible explanation for the inconsistency in NSC drawdown to stress, not tested in this study, is active regulation of NSCs. Although carbon storage is typically modelled as a simple source–sink process (Dietze & Matthes, 2014; Dietze et al., 2014), there is increasing evidence that storage is actively regulated and may be prioritized over growth when carbon is limiting (Herms et al., 1992; Martínez-Vilalta

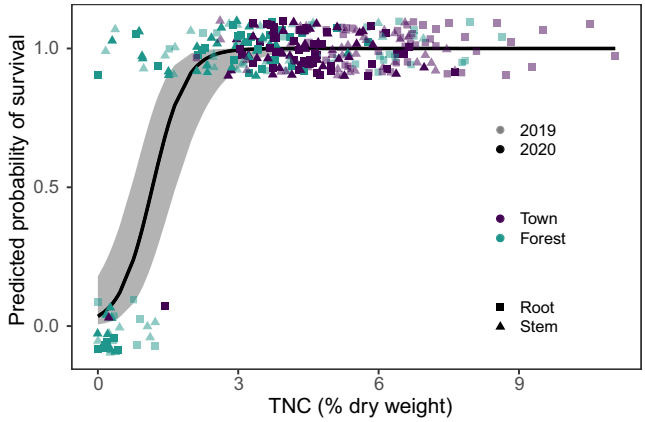

FIGURE 4 Probability of survival predicted by total non-structural carbohydrates (TNC). The line and shading indicate the predicted probability and 95% confidence interval for survival, which quickly approaches 100% above 1.5% TNC. The green and purple points (jittered) indicate the dead (0) and live (1) trees

et al., 2016; Wiley et al., 2017). Genetic variation in NSC regulation (Blumstein & Hopkins, 2020) could underlie the equivocal support for the carbon starvation hypothesis. In addition, many studies focus on seedlings (Galvez et al., 2013; O'Brien et al., 2014; Sapes et al., 2021), which likely differ from adult trees in resource acquisition and storage.

Total NSC stores were lower in the interior forest trees (Forest) than in the forest edge and street trees (Town), and the effect of defoliation on TNC levels was stronger for the Forest trees. This could be because defoliation was milder at the Town site than the Forest, as indicated by the Landsat condition change scores for 2017–2018 (Figure 1). However, the Landsat condition change scores are appropriate for the plot (30 m) scale but did not predict individual-tree defoliation (Figure 1g). Forest edge pixels often include a mix of cover types, which may lead to underestimated defoliation severity if part of the pixel contains cover that is not subject to defoliation. An alternate explanation is that because forest edge trees have higher leaf area and access to light, they have higher NSC levels that are less sensitive to the effects of defoliation than interior forest trees. Furthermore, trees receiving more light may induce more defence compounds such as jasmonic acid (Elderd et al., 2013; Kazan & Manners, 2011), which could add to the edge trees' advantage. If so, our findings suggest that NSC depletion may be a greater risk for interior forests than forest edges, and adds to our growing understanding of how forest edges differ from interior forests (Reinmann & Hutyra, 2017; Reinmann et al., 2020; Smith et al., 2018). In addition, this may help explain why some previous studies (e.g. Wiley et al., 2013) that drew inference from trees growing in a tended garden setting did not find NSC drawdown with defoliation.

4.2 | There is a critical NSC threshold below which mortality occurs

Trees survived with very low TNC reserves. Only trees with root TNC levels below 1.5% dry weight died, and some died with fully depleted (i.e. zero) reserves. This is in contrast to drought (McDowell & Sevanto, 2010; Nelson et al., 2018) or defoliation (Anderegg & Callaway, 2012) studies that showed that mortality occurred without carbon depletion, but bolsters and builds on past work that showed that starch reserves were depleted in trees that died following insect defoliation (Wargo, 1981; Webb, 1981). Most studies of NSC response to defoliation do not include trees that died (McDowell & Sevanto, 2010; Piper & Paula, 2020), and therefore miss threshold dynamics as shown in the present study. Wiley et al. (2016) examined NSC dynamics of lodgepole pines killed by mountain pine beetle, but since the mortality agent was a phloem borer, the mortality process likely differs from defoliation. Unlike early studies that measured only starch (Wargo, 1981; Webb, 1981), our study demonstrates that both starch and sugars, in both stems and roots, were drawn down to near-zero levels before mortality occurred, indicating full depletion of TNC reserves. Whereas starch functions as a storage reservoir, sugars are critical to maintain functions such as osmoregulation and freezing tolerance (Martínez-Vilalta et al., 2016; Sapes et al., 2021), and therefore sugars are a critical component of determining carbon starvation thresholds.

Surprisingly, some surviving trees had TNC reserves below the 1.5% threshold. Similarly, Wargo (1981) found that root starch levels <2% were a necessary, but not sufficient, condition for oak mortality; that is, some trees below that threshold survived. It appears that trees can maintain basic metabolism and osmoregulation at very low levels of TNC, at least for short periods of time. In the present study, however, most of these trees exhibited some canopy dieback and may continue to decline.

5 | CONCLUSIONS

Most ecophysiologically based forest models formalize the concept of carbon starvation to simulate tree mortality in response to non-physical disturbances, such as drought, defoliation and pathogens (Anderegg, Hicke, et al., 2015; Dietze & Matthes, 2014). This includes widely used dynamic vegetation models (DVMs), such as the Community Land Model (Lawrence et al., 2019), PnET (Aber & Federer, 1992; De Bruijn et al., 2014) and the Ecosystem Demography Model (Medvigy et al., 2009), that scientists and policymakers rely on to forecast ecosystem responses to global change (e.g. Thompson et al., 2020). These models all assume that tree mortality is dependent on a full drawdown of carbon stores, an assumption that has until now lacked empirical evidence. Our finding of a 1.5% TNC threshold can improve mortality functions in DVMs and our ability to predict impacts of disturbance.

This study leveraged a unique natural defoliation gradient to demonstrate that defoliated trees drew down their NSC stores, sometimes to zero. Mortality occurred below a threshold of 1.5% TNC. The strong relationships among defoliation, NSC depletion and mortality are in accord with the carbon starvation hypothesis, although, as posited by the tree mortality spiral concept (Franklin et al., 1987; Manion, 1981), carbon starvation may not be the sole

cause of death. Because we were unable to assess tree hydraulics, we could not say that hydraulic failure did not contribute to tree death. The 2016 drought may have caused some cavitation (the blockage of water flow in vessels by air bubbles) and weakened the trees. Since oaks are ring-porous and routinely re-build xylem each spring (Barbaroux & Bréda, 2002), any cavitation that occurred in 2016 would have been unlikely to continue to hamper trees' hydraulic function in subsequent years. However, NSCs are critical for hydraulic function (O'Brien et al., 2014; Sapes et al., 2021), so the NSC depletion we documented here may have impaired hydraulic function. Secondary infection by native insects or diseases is another alternative cause of death of trees weakened by defoliation (Davidson et al., 1999; Wargo, 1996). However, since NSCs are involved in tree defence (Herms et al., 1992), carbon starvation may result in vulnerability to typically innocuous pests (Anderegg & Callaway, 2012). The in situ conditions of this study that included climate stress and more than one year of defoliation demonstrate a realistic scenario in which compounding stressors and disturbance led to decline and mortality. As the direct cause of death or as a precondition, we show that carbon starvation is a key part of the tree mortality spiral.

ACKNOWLEDGEMENTS

Thanks to the Massachusetts DCR -DWSP-Quabbin Reservoir and the Amherst Conservation Commission for site access, and to Greta VanScoy, Nathan Oalican, Samantha Matson, Sofia Kruszka, Emma Conrad-Rooney and Savanna Brown for assistance with field data collection. Meghan Graham MacLean identified potential Forest plot locations, and Artemis Roehrig established the Town tree locations. Manisha Patel facilitated laboratory access during the Covid-19 pandemic. Meghan Graham MacLean and Bethany Bradley provided analytic advice and they, along with two anonymous reviewers, provided valuable feedback on the manuscript. Funding for this project was from the National Science Foundation (RAPID 1926052, REU Site 1459519 and the Harvard Forest LTER 1832210).

CONFLICT OF INTEREST

The authors declare no conflict of interest.

AUTHORS' CONTRIBUTIONS

A.B.P., M.B., J.S.E. and J.R.T. designed the research; A.B.P., M.B., D.L. and J.L.C. collected the field data; M.B. and D.L. performed the laboratory analyses; V.J.P. designed and conducted the Landsat defoliation analysis; A.B.P. led the data analysis and manuscript writing; all authors contributed to editing the manuscript.

DATA AVAILABILITY STATEMENT

Data associated with this experiment are available on the Harvard Forest Data Archive (https://harvardforest.fas.harvard.edu/harvard-forest-data-archive; HF369), and are openly available through this local archive as well as the Environmental Data Initiative (https://portal.edirepository.org/nis/home.jsp; https://doi.org/10.6073/pasta/caf757bc4d0d0509bfc16fc98db9a927).

ORCID

Audrey Barker Plotkin https://orcid.org/0000-0002-4473-9785
Meghan Blumstein https://orcid.org/0000-0003-0905-6265
Valerie J. Pasquarella https://orcid.org/0000-0003-1258-6195
Jennifer L. Chandler https://orcid.org/0000-0002-7266-520X
Jonathan R. Thompson https://orcid.org/0000-0003-0512-1226

REFERENCES

Aber, J. D., & Federer, C. A. (1992). A generalized, lumped-parameter model of photosynthesis, evapotranspiration and net primary production in temperate and boreal forest ecosystems. *Oecologia*, *92*(4), 463–474. https://doi.org/10.1007/BF00317837

Adams, H. D., Zeppel, M. J. B., Anderegg, W. R. L., Hartmann, H., Landhäusser, S. M., Tissue, D. T., Huxman, T. E., Hudson, P. J., Franz, T. E., Allen, C. D., Anderegg, L. D. L., Barron-Gafford, G. A., Beerling, D. J., Breshears, D. D., Brodribb, T. J., Bugmann, H., Cobb, R. C., Collins, A. D., Dickman, L. T., … McDowell, N. G. (2017). A multi-species synthesis of physiological mechanisms in drought-induced tree mortality. *Nature Ecology & Evolution*, *1*(9), 1285–1291. https://doi.org/10.1038/s41559-017-0248-x

Anderegg, W. R. L., & Callaway, E. S. (2012). Infestation and hydraulic consequences of induced carbon starvation. *Plant Physiology*, *159*(4), 1866–1874. https://doi.org/10.1104/pp.112.198424

Anderegg, W. R. L., Hicke, J. A., Fisher, R. A., Allen, C. D., Aukema, J., Bentz, B., Hood, S., Lichstein, J. W., Macalady, A. K., McDowell, N., Pan, Y., Raffa, K., Sala, A., Shaw, J. D., Stephenson, N. L., Tague, C., & Zeppel, M. (2015). Tree mortality from drought, insects, and their interactions in a changing climate. *New Phytologist*, *208*(June), 674–683. https://doi.org/10.1111/nph.13477

Anderegg, W. R. L., Schwalm, C., Biondi, F., Camarero, J. J., Koch, G., Litvak, M., Ogle, K., Shaw, J. D., Shevliakova, E., Williams, A. P., Wolf, A., Ziaco, E., & Pacala, S. (2015). Pervasive drought legacies in forest ecosystems and their implications for carbon cycle models. *Science*, *349*(6247), 528–532. https://doi.org/10.1126/science.aab1833

Aukema, J. E., McCullough, D. G., Holle, B. V., Liebhold, A. M., Britton, K., & Frankel, S. J. (2010). Historical accumulation of nonindigenous forest pests in the continental United States. *BioScience*, *60*(11), 886–897. https://doi.org/10.1525/bio.2010.60.11.5

Barbaroux, C., & Bréda, N. (2002). Contrasting distribution and seasonal dynamics of carbohydrate reserves in stem wood of adult ring-porous sessile oak and diffuse-porous beech trees. *Tree Physiology*, *22*(17), 1201–1210. https://doi.org/10.1093/treephys/22.17.1201

Blumstein, M., & Hopkins, R. (2020). Adaptive variation and plasticity in nonstructural carbohydrate storage in a temperate tree species. *Plant, Cell & Environment*, *2020*, 1–12. https://doi.org/10.1111/pce.13959

Boose, E. R., & Gould, E. (2019). *Harvard forest climate data since 1964*. Harvard Forest Data Archive HF300. Retrieved from https://harvardforest1.fas.harvard.edu/exist/apps/datasets/showData.html?id=HF300

Brooks, M. E., Kristensen, K., van Benthem, K. J., Magnusson, A., Berg, C. W., Nielsen, A., Skaug, H. J., Maechler, M., & Bolker, B. M. (2017). glmmTMB balances speed and flexibility among packages for zero-inflated generalized linear mixed modeling. *The R Journal*, *9*(2), 378–400. https://doi.org/10.32614/RJ-2017-066

Brown, S. (2019). The very hungry, lonely, and sick caterpillar: Exploring pathogen occurrence within low-density populations of gypsy moth. *Harvard Forest Summer Research Program in Ecology 27th Annual Student Symposium*, 7.

Campbell, R. W., & Sloan, R. J. (1977). Forest stand responses to defoliation by the gypsy moth. *Forest Science*, *23*(Supplement 2), a0001–z0001.

Cavender-Bares, J. (2019). Diversification, adaptation, and community assembly of the American oaks (*Quercus*), a model clade for

integrating ecology and evolution. *New Phytologist*, *221*(2), 669–692. https://doi.org/10.1111/nph.15450

Cohen W. B., Yang Z., Stehman S. V., Schroeder T. A., Bell D. M., Masek J. G., Huang C., Meigs G. W. (2016). Forest disturbance across the conterminous United States from 1985–2012: The emerging dominance of forest decline. *Forest Ecology and Management*, *360*, 242–252. https://doi.org/10.1016/j.foreco.2015.10.042

Conrad-Rooney, E., Barker Plotkin, A., Pasquarella, V. J., Elkinton, J., Chandler, J. L., & Matthes, J. H. (2020). Defoliation severity is positively related to soil solution nitrogen availability and negatively related to soil nitrogen concentrations following a multi-year invasive insect irruption. *AoB PLANTS*, *12*(6), 1–9. https://doi.org/10.1093/aobpla/plaa059

Davidson, C. B., Gottschalk, K. W., & Johnson, J. E. (1999). Tree mortality following defoliation by the European gypsy moth (*Lymantria dispar* L.) in the United States: A review. *Forest Science*, *45*(1), 74–84. https://doi.org/10.1093/forestscience/45.1.74

De Bruijn, A., Gustafson, E. J., Sturtevant, B. R., Foster, J. R., Miranda, B. R., Lichti, N. I., & Jacobs, D. F. (2014). Toward more robust projections of forest landscape dynamics under novel environmental conditions: Embedding PnET within LANDIS-II. *Ecological Modelling*, *287*, 44–57. https://doi.org/10.1016/j.ecolmodel.2014.05.004

Dietze, M. C., & Matthes, J. H. (2014). A general ecophysiological framework for modelling the impact of pests and pathogens on forest ecosystems. *Ecology Letters*, *17*(11), 1418–1426. https://doi.org/10.1111/ele.12345

Dietze, M. C., Sala, A., Carbone, M. S., Czimczik, C. I., Mantooth, J. A., Richardson, A. D., & Vargas, R. (2014). Nonstructural carbon in woody plants. *Annual Review of Plant Biology*, *65*, 667–687. https://doi.org/10.1146/annurev-arplant-050213-040054

Douma, J. C., & Weedon, J. T. (2019). Analysing continuous proportions in ecology and evolution: A practical introduction to beta and Dirichlet regression. *Methods in Ecology and Evolution*, *10*(9), 1412–1430. https://doi.org/10.1111/2041-210X.13234

Elderd, B. D., Rehill, B. J., Haynes, K. J., & Dwyer, G. (2013). Induced plant defenses, host-pathogen interactions, and forest insect outbreaks. *Proceedings of the National Academy of Sciences of the United States of America*, *110*(37), 14978–14983. https://doi.org/10.1073/pnas.1300759110

Elkinton, J. S., Bittner, T. D., Pasquarella, V. J., Boettner, G. H., Liebhold, A. M., Gould, J. R., Faubert, H., Tewksbury, L., Broadley, H. J., Havill, N. P., Hajek, A. E., & Ross, D. (2019). Relating aerial deposition of Entomophaga maimaiga conidia (Zoopagomycota: Entomophthorales) to mortality of gypsy moth (Lepidoptera: Erebidae) larvae and nearby defoliation. *Environmental Entomology*, *48*(5), 1214–1222. https://doi.org/10.1093/ee/nvz091

Elkinton, J. S., & Liebhold, A. M. (1990). Population dynamics of gypsy moth in North America. *Annual Review of Entomology*, *35*, 571–596. https://doi.org/10.1146/annurev.en.35.010190.003035

Fei, S., Morin, R. S., Oswalt, C. M., & Liebhold, A. M. (2019). Biomass losses resulting from insect and disease invasions in US forests. *Proceedings of the National Academy of Sciences of the United States of America*, *116*(35), 17371–17376. https://doi.org/10.1073/pnas.1820601116

Finzi, A. C., Giasson, M.-A., Barker Plotkin, A. A., Aber, J. D., Boose, E. R., Davidson, E. A., Dietze, M. C., Ellison, A. M., Frey, S. D., Goldman, E., Keenan, T. F., Melillo, J. M., Munger, J. W., Nadelhoffer, K. J., Ollinger, S. V., Orwig, D. A., Pederson, N., Richardson, A. D., Savage, K., … Foster, D. R. (2020). Carbon budget of the Harvard Forest Long-Term Ecological Research site: Pattern, process, and response to global change. *Ecological Monographs*, *90*(4), 1–37. https://doi.org/10.1002/ecm.1423

Foster, J. R. (2017). Xylem traits, leaf longevity and growth phenology predict growth and mortality response to defoliation in northern temperate forests. *Tree Physiology*, *37*(9), 1151–1165. https://doi.org/10.1093/treephys/tpx043

Franklin, J. F., Shugart, H. H., Harmon, M. E., Franklin, J. F., Shugart, H. H., & Harmon, M. E. (1987). Tree Death as an Ecological Process: The causes, consequences, and variability of tree mortality. *BioScience*, *37*(8), 550–556. https://doi.org/10.1016/B978-0-12-386525-0.00058-5

Furze, M. E., Huggett, B. A., Aubrecht, D. M., Stolz, C. D., Carbone, M. S., & Richardson, A. D. (2018). Whole-tree nonstructural carbohydrate storage and seasonal dynamics in five temperate species. *New Phytologist*, *221*, 1466–1477. https://doi.org/10.1111/nph.15462

Galvez, D. A., Landhäusser, S. M., & Tyree, M. T. (2013). Low root reserve accumulation during drought may lead to winter mortality in poplar seedlings. *New Phytologist*, *198*(1), 139–148. https://doi.org/10.1111/nph.12129

Gandhi, K. J. K., & Herms, D. A. (2010). Direct and indirect effects of alien insect herbivores on ecological processes and interactions in forests of eastern North America. *Biological Invasions*, *12*(2), 389–405. https://doi.org/10.1007/s10530-009-9627-9

Hartig, F. (2020). *DHARMa: Residual diagnostics for hierarchical (multi-level/mixed) regression models*. R package version 0.3.0.

Hartmann, H., & Trumbore, S. (2016). Understanding the roles of nonstructural carbohydrates in forest trees – From what we can measure to what we want to know. *The New Phytologist*, *211*(2), 386–403. https://doi.org/10.1111/nph.13955

Heichel, G. H., & Turner, N. C. (1983). CO_2 assimilation of primary and regrowth foliage of red maple (*Acer rubrum* L.) and red oak (*Quercus rubra* L.): Response to defoliation. *Oecologia*, *57*(1–2), 14–19. https://doi.org/10.1007/BF00379555

Herms, D. A., Mattson, W. J., North, U., Forest, C., Station, E., & Lansing, E. (1992). The dilemma of plants: To grow or defend. *The Quarterly Review of Biology*, *67*(3), 283–335. https://doi.org/10.1086/417659

Kazan, K., & Manners, J. M. (2011). The interplay between light and jasmonate signalling during defence and development. *Journal of Experimenta Botany*, *62*, 4087–4100. https://doi.org/10.1093/jxb/err142

Koch, F. H., & Coulton, J. W. (2018). Drought and moisture surplus patterns in the conterminous United States: 2017, 2015-2017, and 2013-2017. In K. M. Potter & B. L. Conkling (Eds.), *Forest health monitoring: National status, trends, and analysis* (pp. 77–96). U.S. Department of Agriculture, Forest Service, Southern Research Station.

Kulman, H. M. (1971). Effects of insect defoliation on growth and mortality of trees. *Annual Review of Entomology*, *16*(1), 289–324. https://doi.org/10.1146/annurev.en.16.010171.001445

Landhäusser, S. M., Chow, P. S., Dickman, L. T., Furze, M. E., Kuhlman, I., Schmid, S., Wiesenbauer, J., Wild, B., Gleixner, G., Hartmann, H., Hoch, G., McDowell, N. G., Richardson, A. D., Richter, A., & Adams, H. D. (2018). Standardized protocols and procedures can precisely and accurately quantify non-structural carbohydrates. *Tree Physiology*, *38*, 1764–1778. https://doi.org/10.1093/treephys/tpy118

Landhäusser, S. M., & Lieffers, V. J. (2003). Seasonal changes in carbohydrate reserves in mature northern *Populus tremuloides* clones. *Trees – Structure and Function*, *17*(6), 471–476. https://doi.org/10.1007/s00468-003-0263-1

Landhäusser, S. M., & Lieffers, V. J. (2012). Defoliation increases risk of carbon starvation in root systems of mature aspen. *Trees – Structure and Function*, *26*(2), 653–661. https://doi.org/10.1007/s00468-011-0633-z

Lawrence, D. M., Fisher, R. A., Koven, C. D., Oleson, K. W., Swenson, S. C., Bonan, G., Collier, N., Ghimire, B., Kampenhout, L., Kennedy, D., Kluzek, E., Lawrence, P. J., Li, F., Li, H., Lombardozzi, D., Riley, W. J., Sacks, W. J., Shi, M., Vertenstein, M., … Zeng, X. (2019). The community land model version 5: Description of new features, benchmarking, and impact of forcing uncertainty. *Journal of Advances in Modeling Earth Systems*, *11*(12), 4245–4287. https://doi.org/10.1029/2018MS001583

Liebhold, A., Elkinton, J., Williams, D., & Muzika, R. M. (2000). What causes outbreaks of the gypsy moth in North America? *Population Ecology*, *42*(3), 257–266. https://doi.org/10.1007/PL00012004

Liebhold, A. M., Mccullough, D. G., Blackburn, L. M., Frankel, S. J., Von Holle, B., & Aukema, J. E. (2013). A highly aggregated geographical distribution of forest pest invasions in the USA. *Diversity and Distributions*, *19*(9), 1208–1216. https://doi.org/10.1111/ddi.12112

Lindroth, R. L., Klein, K. A., Hemming, J. D. C., & Feuker, A. M. (1997). Variation in temperature and dietary nitrogen affect performance of the gypsy moth (*Lymantria dispar* L.). *Physiological Entomology*, *22*(1), 55–64. https://doi.org/10.1111/j.1365-3032.1997.tb01140.x

Lovett, G. M., Christenson, L. M., Groffman, P. M., Jones, C. G., Hart, J. E., & Mitchell, M. J. (2002). Insect defoliation and nitrogen cycling in forests. *BioScience*, *52*(4), 335–341. https://doi.org/10.1641/0006-3568(2002)052%5B0335:IDANCI%5D2.0.CO;2

Lovett, G. M., Weiss, M., Liebhold, A. M., Holmes, T. P., Leung, B., Lambert, K. F., Orwig, D. A., Campbell, F. T., Rosenthal, J., McCullough, D. G., Wildova, R., Ayres, M. P., Canham, C. D., Foster, D. R., LaDeau, S. L., & Weldy, T. (2016). Nonnative forest insects and pathogens in the United States: Impacts and policy options. *Ecological Applications*, *26*(5), 1437–1455. https://doi.org/10.1890/15-1176

Lüdecke, D. (2018). ggeffects: Tidy data frames of marginal effects from regression models. *Journal of Open Source Software*, *3*(26), 772. https://doi.org/10.21105/joss.00772

Manion, P. D. (1981). *Tree disease concepts*. Prentice Hall Inc.

Martínez-Vilalta, J., Sala, A., Asensio, D., Galiano, L., Hoch, G., Palacio, S., Piper, F. I., & Lloret, F. (2016). Dynamics of non-structural carbohydrates in terrestrial plants: A global synthesis. *Ecological Monographs*, *86*(4), 495–516. https://doi.org/10.1002/ecm.1231

McDowell, N. G., Pockman, W. T., Allen, C. D., David, D., Cobb, N., Kolb, T., Plaut, J., Sperry, J., West, A., Williams, D. G., & Yepez, E. A. (2008). Mechanisms of plant survival and mortality during drought: Why do some plants survive while others succumb to drought? *New Phytologist*, *178*, 719–739.

McDowell, N. G., & Sevanto, S. (2010). Commentary: The mechanisms of carbon starvation: How, when, or does it even occur at all? *New Phytologist*, *186*, 264–266. https://doi.org/10.1111/j.1469-8137.2010.03232.x

Medvigy, D., Wofsy, S. C., Munger, J. W., Hollinger, D. Y., & Moorcroft, P. R. (2009). Mechanistic scaling of ecosystem function and dynamics in space and time: Ecosystem Demography model version 2. *Journal of Geophysical Research: Biogeosciences*, *114*(1), 1–21. https://doi.org/10.1029/2008JG000812

Millar, C. I., & Stephenson, N. L. (2015). Temperate forest health in an era of emerging megadisturbance. *Science*, *349*(6250), 823–826. https://doi.org/10.1126/science.aaa9933

Nelson, R. G., Rutherford, J. N., Hinde, K., Clancy, K. B. H., Ellison, A. M., LeRoy, C. J., Landsbergen, K. J., Bosanquet, E., Borden, D. B., CaraDonna, P. J., Cheney, K., Crystal-Ornelas, R., DeFreece, A., Goralnik, L., Irons, E., Merkle, B. G., O'Connell, K. E. B., Penick, C. A., Rustad, L., … Davies, T. J. (2018). Xylem traits, leaf longevity and growth phenology predict growth and mortality response to defoliation in northern temperate forests. *New Phytologist*, *37*(1), 1–13. https://doi.org/10.1093/biosci/biw005

O'Brien, M. J., Leuzinger, S., Philipson, C. D., Tay, J., & Hector, A. (2014). Drought survival of tropical tree seedlings enhanced by non-structural carbohydrate levels. *Nature Climate Change*, *4*(8), 710–714. https://doi.org/10.1038/nclimate2281

Palacio, S., Hernández, R., Maestro-Martínez, M., & Camarero, J. J. (2012). Fast replenishment of initial carbon stores after defoliation by the pine processionary moth and its relationship to the re-growth ability of trees. *Trees – Structure and Function*, *26*(5), 1627–1640. https://doi.org/10.1007/s00468-012-0739-y

Pasquarella, V. J. (2018). Landsat-based gypsy moth defoliation assessment (Southern New England), (version 3.0). *Zenodo*, https://doi.org/10.5281/zenodo.1163679

Pasquarella, V. J., Bradley, B. A., & Woodcock, C. E. (2017). Near-real-time monitoring of insect defoliation using Landsat time series. *Forests*, *8*(8), 275. https://doi.org/10.3390/f8080275

Pasquarella, V. J., Elkinton, J. S., & Bradley, B. A. (2018). Extensive gypsy moth defoliation in Southern New England characterized using Landsat satellite observations. *Biological Invasions*, *20*(11), 3047–3053. https://doi.org/10.1007/s10530-018-1778-0

Pasquarella, V. J., Mickley, J. G., Barker Plotkin, A., Maclean, R. G., Anderson, R. M., Brown, L. M., Wagner, D. L., Singer, M. S., & Bagchi, R. (2021). Predicting defoliator abundance and defoliation measurements using Landsat-based condition scores. *Remote Sensing in Ecology and Conservation*, 1–18, in press. https://doi.org/10.1002/rse2.211

Piper, F. I., Gundale, M. J., & Fajardo, A. (2015). Extreme defoliation reduces tree growth but not C and N storage in a winter-deciduous species. *Annals of Botany*, *115*(7), 1093–1103. https://doi.org/10.1093/aob/mcv038

Piper, F. I., & Paula, S. (2020). The role of nonstructural carbohydrates storage in forest resilience under climate change. *Current Forestry Reports*, *6*(1), 1–13. https://doi.org/10.1007/s40725-019-00109-z

R Core Team. (2019). *R: A language and environment for statistical computing*. R Foundation for Statistical Computing. Retrieved from https://www.r-project.org/

Reinmann, A. B., & Hutyra, L. R. (2017). Edge effects enhance carbon uptake and its vulnerability to climate change in temperate broadleaf forests. *Proceedings of the National Academy of Sciences of the United States of America*, *114*(1), 107–112. https://doi.org/10.1073/pnas.1612369114

Reinmann, A. B., Smith, I. A., Thompson, J. R., & Hutyra, L. R. (2020). Urbanization and fragmentation mediate temperate forest carbon cycle response to climate. *Environmental Research Letters*, *15*(11), 114036. https://doi.org/10.1088/1748-9326/abbf16

Richardson, A. D., Carbone, M. S. M., Keenan, T. F. T., Czimczik, C. C. I., Hollinger, D. D. Y., Murakami, P., Schaberg, P. G. P., & Xu, X. (2013). Seasonal dynamics and age of stemwood nonstructural carbohydrates in temperate forest trees. *New Phytologist*, *197*, 850–861. https://doi.org/10.1111/nph.12042

Sala, A., & Hoch, G. (2009). Height-related growth declines in ponderosa pine are not due to carbon limitation. *Plant, Cell and Environment*, *32*(1), 22–30. https://doi.org/10.1111/j.1365-3040.2008.01896.x

Sapes, G., Demaree, P., Lekberg, Y., & Sala, A. (2021). Plant carbohydrate depletion impairs water relations and spreads via ectomycorrhizal networks. *New Phytologist*, *229*(6), 3172–3183. https://doi.org/10.1111/nph.17134

Schmid, S., Palacio, S., & Hoch, G. (2017). Growth reduction after defoliation is independent of CO_2 supply in deciduous and evergreen young oaks. *New Phytologist*, *214*(4), 1479–1490. https://doi.org/10.1111/nph.14484

Smith, I. A., Hutyra, L. R., Reinmann, A. B., Marrs, J. K., & Thompson, J. R. (2018). Piecing together the fragments: Elucidating edge effects on forest carbon dynamics. *Frontiers in Ecology and the Environment*, *16*(4), 213–221. https://doi.org/10.1002/fee.1793

Thompson, J. R., Laflower, D., Plisinski, J. S., MacLean, M. G., & (2020). *Land sector report: A technical report of the Massachusetts 2050 decarbonization roadmap study* (issue December). Commonwealth of Massachusetts Executive Office of Energy and Environmental Affairs.

Tixier, A., Orozco, J., Roxas, A. A., Earles, J. M., & Zwieniecki, M. A. (2018). Diurnal variation in nonstructural carbohydrate storage in trees: Remobilization and vertical mixing. *Plant Physiology*, *178*(4), 1602–1613. https://doi.org/10.1104/pp.18.00923

Wargo, P. M. (1981). Defoliation and tree growth. In C. C. Doane & M. L. McManus (Eds.), *The gypsy moth: Research toward integrated pest management* (pp. 225–240). USDA For. Serv. Tech. Bull. 1584.

Wargo, P. M. (1996). Consequences of environmental stress on oak: Predisposition to pathogens. *Annales Des Sciences Forestieres*, *53*(2–3), 359–368. https://doi.org/10.1051/forest:19960218

Webb, W. L. (1981). Relation of starch content to conifer mortality and growth loss after defoliation by the Douglas-fir Tussock moth. *Forest Science*, *27*, 224–232.

Wiley, E., Casper, B. B., & Helliker, B. R. (2017). Recovery following defoliation involves shifts in allocation that favour storage and reproduction over radial growth in black oak. *Journal of Ecology*, *105*(2), 412–424. https://doi.org/10.1111/1365-2745.12672

Wiley, E., Huepenbecker, S., Casper, B. B., & Helliker, B. R. (2013). The effects of defoliation on carbon allocation: Can carbon limitation reduce growth in favour of storage? *Tree Physiology*, *33*(11), 1216–1228. https://doi.org/10.1093/treephys/tpt093

Wiley, E., Rogers, B. J., Hodgkinson, R., & Landhäusser, S. M. (2016). Nonstructural carbohydrate dynamics of lodgepole pine dying from mountain pine beetle attack. *New Phytologist*, *209*(2), 550–562. https://doi.org/10.1111/nph.13603

SUPPORTING INFORMATION

Additional Supporting Information may be found online in the Supporting Information section.

How to cite this article: Barker Plotkin, A., Blumstein, M., Laflower, D., Pasquarella, V. J., Chandler, J. L., Elkinton, J. S., & Thompson, J. R. (2021). Defoliated trees die below a critical threshold of stored carbon. *Functional Ecology*, 35, 2156–2167. https://doi.org/10.1111/1365-2435.13891